ELSEVIER

Journal of Nuclear Materials 246 (1997) 150–157

journal of nuclear materials

Solubility of magnesium in uranium dioxide

Takeo Fujino [a,*], Shohei Nakama [a], Nobuaki Sato [a], Kohta Yamada [a], Kousaku Fukuda [b], Hiroyuki Serizawa [b], Tetsuo Shiratori [b]

[a] *Institute for Advanced Materials Processing, Tohoku University, 2-1-1 Katahira, Aoba-ku, Sendai 980-77, Japan*
[b] *Japan Atomic Energy Research Institute, Tokai Research Establishment, Tokai-mura, Naka-gun, Ibaraki-ken 319-11, Japan*

Received 26 April 1996; accepted 30 April 1997

Abstract

The solubility of magnesium in uranium dioxide under low oxygen pressures was studied at 1200°C. Magnesium was found to dissolve up to $y > 0.1$ (and below $y = 0.15$) of the apparent formula, $Mg_yU_{1-y}O_{2+x}$ ($x \lessgtr 0$) on heating at $p_{O_2} = 10^{-15}$ and $\leq 10^{-19}$ atm. The formed solid solution in such a low p_{O_2} region was of the type $(Mg_aU_{1-a})\{Mg_b\}O_{2+c}$, in which the magnesium atoms partly occupy the interstitial sites together with the substitutional sites for uranium atoms. The ratio of interstitial atoms to the total magnesium atoms increased from 0.23 ($y = 0.05$) or 0.39 ($y = 0.1$) at $p_{O_2} = 10^{-15}$ atm with decreasing oxygen partial pressure to 0.62–0.63 ($y = 0.05$ and 0.1) at $p_{O_2} \leq 10^{-19}$ atm. The lattice parameter of the $(Mg_aU_{1-a})\{Mg_b\}O_{2+c}$ solid solutions was represented as a linear equation of a, b and c. The interstitial magnesium caused an increase in the lattice parameter, in contrast to the substitutional magnesium which largely decreases the lattice parameter. It is possible that the uranium atoms in the solid solutions prepared at low oxygen partial pressures ($\leq 10^{-19}$ atm) were reduced to slightly less than the tetravalent state. © 1997 Elsevier Science B.V.

1. Introduction

Some kinds of UO_2–metal oxide solid solutions are expected to give better fuel performance. The change of thermodynamic, chemical and/or transport properties from undoped UO_2 fuel could cause the elongation of fuel life up to economically eligible high burnups. It has been reported that the solid solutions formed by the addition of small amounts of niobium [1–3], titanium [3,4] or chromium [5] to UO_2 exhibit increased grain size in the pellet. Large-grained UO_2 doped with magnesium reduced the fission gas release of undoped UO_2 to 40% [6]. Oxygen potentials of UO_2 doped with niobium [7] and titanium [8] have been measured.

Solid solutions of some lower valence (+2 or +3) metals M, $M_yU_{1-y}O_{2+x}$, exhibit thermodynamic properties which are considerably changed from UO_{2+x}. The $Mg_yU_{1-y}O_{2+x}$ ($x \lessgtr 0$) solid solution containing divalent magnesium has a considerably wide existence range of oxygen hypostoichiometry ($x < 0$) [9,10] together with hyperstoichiometry [11,12]. On increasing the value of x of $Mg_yU_{1-y}O_{2+x}$ from the lowest negative one, the oxygen potential of the solid solution is supposed to increase first slowly with x. The rate of the increase becomes gradually higher with increasing x. Around a certain negative x value, which changes depending on y, the oxygen potential very rapidly increases with increasing x. After passing through this point, the increase rate of the oxygen potential subsides as x still increases. In the case of such an x dependence of the oxygen potential, the irradiation behavior should be improved if the fully reduced magnesium solid solution is used as fuel, since its oxygen potential is considered to remain low values for long period of irradiation although the x value increases. The concentration of magnesium in the solid solution is important for this effect. However, there have been some inconsistencies in the reports about the solubility of magnesium in UO_2 under very low oxygen pressures.

Magnesium dissolves in UO_2 up to $y = 0.33$ if the oxygen pressure, p_{O_2}, is high enough [13,14]. However,

* Corresponding author. Tel.: +81-22 217 5163; fax: +81-22 217 5164.

PII S0022-3115(97)00143-8

the solubility lowers as the x value decreases in the hypostoichiometric region under lower p_{O_2}. Anderson and Johnson [15] have observed that the solubility was only a few mol% when MgO was heated with UO_2 in vacuum at 2350°C. The present authors [16] obtained the result that the solubility was 2 mol% in a H_2 atmosphere at 1300°C. The lattice parameter versus y plot for nominal $Mg_yU_{1-y}O_{2+x}$ ($x < 0$) solid solution showed a break at $y = 0.02$. However, in another study [17] on the solubility of magnesium for the heated sample in H_2 using the transmission electron microscope (TEM) technique, MgO was observed still below $y = 0.01$, namely the solubility was less than 1 mol%.

The aim of this work is to clarify the solubility limit of magnesium in strongly reducing atmospheres at 1200°C. It was thought that the dissolution was related to the low diffusion rate of magnesium in UO_2 lattice for the formation reaction of solid solution. Therefore, to obtain the sample of good homogeneity, the cycle of the grinding and heating process was repeated five to seven times in preparation of the specimens. The crystal and defect structures and the phase analysis of the products were carried out by X-ray powder diffractometry and density measurement after chemical analysis of the oxygen non-stoichiometry.

2. Experimental

2.1. Materials

Uranium metal turnings were degreased with acetone, washed with water and dissolved in 6 M nitric acid. Uranium was then extracted into TBP (organic phase) from the acid. After washing the organic phase with nitric acid, uranium was scrubbed into water and succeedingly into dilute ammonium carbonate solution. The precipitation of ammonium diuranate was obtained by the addition of ammonium hydroxide solution. After filtration, this compound was converted to UO_3 by heating in air at 500°C [18]. Stoichiometric uranium dioxide was obtained by heating UO_3 in a stream of hydrogen at 1000°C for 6 h. The main metallic impurities in the UO_2 analyzed by the ICP method are shown in Table 1.

Guaranteed reagent heavy MgO (Ca < 0.05%, heavy metals < 0.005%) was purchased from Wako Pure Chemicals Industries Co. Hydrogen (99.999%) and N_2 (99.99%) gases were obtained from Nippon Sanso Co., and used after the impurity oxygen and moisture were removed by passing through a hot copper tube and then a liquid nitrogen trap. Carbon dioxide (99.99%), obtained from the same supplier, was used as received.

Table 1
Metallic impurities in UO_2

Element	Amount (ppm)
Pd	54
Y	2
La	4
Tm	94
Th	4

2.2. Sample preparation

Calculated amounts of UO_2 and MgO or $MgUO_4$ [19] were weighed and intimately mixed in an agate mortar for 30 min. The mixture was heated in a muffle furnace in air at 800°C for ~ 70 h. After cooling to room temperature, the product was ground and heated again under the same conditions. This cycle was repeated three times.

The air heated product (about 1 g) was pressed into 7 mm ∅ pellet at 250 MPa. The pellets were placed on an alumina boat and they were heated in a horizontal SiC tube furnace in a stream of CO_2/H_2 mixed gases at 1200°C for ~ 50 h. The mixing ratio of the gases was controlled by two mass-flow controllers (Kofloc, Type-3510 1/4SW-500SCCM and 1/4-10SCCM) equipped for each gas. The oxygen partial pressure of the mixed gas was checked by an oxygen monitor with non-stoichiometric barium titanate probe [20]. After cooling, the pellets were crushed and mixed. The powder was again pressed into pellets and heated under the same conditions. This cycle was repeated five to seven times. In the last two cycles of mixing and heating, the sample pellets were heated in a stream of either H_2 ($p_{O_2} \leq 10^{-19}$ atm) or CO_2/H_2 mixed gases with intended oxygen partial pressures.

2.3. Chemical analysis

About 20 mg of the powdered oxide sample was precisely weighed and dissolved in 1.5 M sulfuric acid containing an excess of Ce(IV). The x value of the solid solution, $Mg_yU_{1-y}O_{2+x}$, was determined by the cerium back-titration method [21,22], which consists of titration of the excess Ce(IV) by standard Fe(II) ammonium sulfate solution with ferroin indicator. The error of the x value was estimated to be within ± 0.005.

2.4. X-ray diffraction analysis

X-ray powder diffractometry was carried out with a Rigaku Type RAD-IC diffractometer using Cu Kα radiation (40 kV, 20 mA) monochromatized with curved pyrolytic graphite. The slit system used was 1°–0.5 mm–1°–0.15 mm. The scanning was carried out in the range $10° \leq 2\theta \leq 140°$. The scanning rate was usually $1°(2\theta)$/min, but for close examination of the precipitation of MgO phase, the rate was lowered to $0.05°(2\theta)$/min or step scanning was adopted with a 36 s counting time. The least-squared calculation of lattice parameters was carried out by the LCR2 program [23].

2.5. Density measurement

The density of the solid solution was measured by the toluene displacement method. An amount of powder of about 3 g was measured in a glass bulb (7.423 g in weight with 2.861 ml inner volume) first in air and then in toluene at 25°C. To minimize the systematic error from open pores in the powder sample, the bulb containing the sample and toluene was put in a desiccator and evacuated until the bubble formation from the open pores ceased.

3. Results and discussion

The X-ray powder diffraction patterns for the reaction products of $y = 0$, 0.02, 0.05 and 0.1 in the atmospheres of both $p_{O_2} = 10^{-15}$ and $\leq 10^{-19}$ atm showed that they were all of face-centered cubic UO_2 structure. The oxygen partial pressure in the purified H_2 stream, which is supposed to be lower than 10^{-19} atm, was given by the inequality since calibration of the barium titanate monitor was made by the mixed gas of CO_2/H_2. The X-ray patterns contained no other peaks of precipitated phases with the exception of the $y = 0.15$ sample, for which the strongest peak of MgO was detected at 42.83° although the peak intensities of this phase were very weak. This peak will be discussed later in this paper.

Fig. 1 shows the change of x of $Mg_yU_{1-y}O_{2+x}$ with y value for the samples heated in strong reducing atmospheres at 1200° for 50 h. In Fig. 1, the circles and triangles show the different runs of experiment in a stream of H_2 ($p_{O_2} \leq 10^{-19}$ atm). It is seen that the x value decreases with increasing y. The square marks indicate the run at $p_{O_2} = 10^{-15}$ atm. No significant discrepancies are seen in the x values for $p_{O_2} = 10^{-15}$ atm and $\leq 10^{-19}$ atm, showing that the x increase due to the p_{O_2} increase is smaller than the error in the x determination. Now if we connect $x = 0$ at $y = 0$ with the x value of -0.15 at $y = 0.15$, the slope is obtained as -1, i.e., $x = -y$. This slope implies that each Mg^{2+} ion dissolves in the UO_2 lattice accompanied by one O^{2-} and one V_O (oxygen vacancy). The solid solution formed can be expressed as $Mg_y^{2+}U_{1-y}^{4+}O_{2-y}^{2-}(V_O)_y$, which indicates that the uranium atoms remain tetravalent state in the solid solution without any oxidation to a higher valence state. This result at first sight does not seem to be in harmony with the knowledge on the mixed oxides of uranium with other metals that uranium tends to take on higher valence states and that the known most reduced state of uranium in oxides, i.e., tetravalency, is rather difficult to be attained in the mixed oxides (solid solutions and ternary uranium compounds) in reducing atmosphere. For example, $BaUO_{3+x}$ [24] and $Sr_2(La_{1-3x}Sr_{2x}U_x^{5+})U^{5+}O_6$ [25] have been reported to form by heating in H_2 streams at 1100°C. These chemical formulas show that the mean uranium valence is still higher than +4 even in a strong reducing atmosphere of H_2. The difference is assumed to be because our samples were heated at a higher temperature of 1200°C with lower

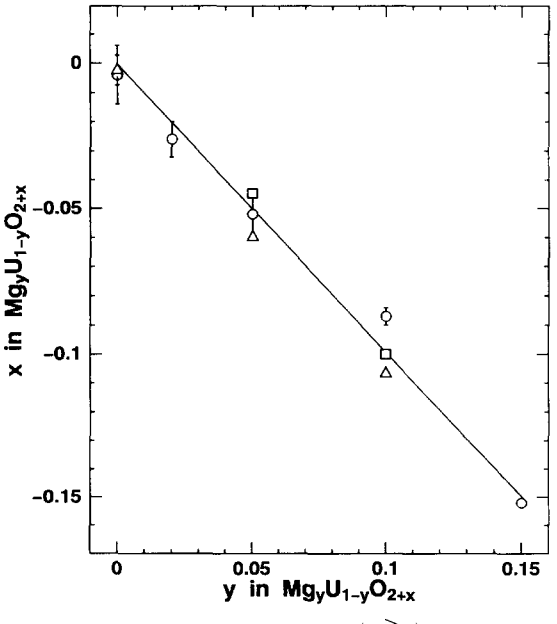

Fig. 1. Change of x of $Mg_yU_{1-y}O_{2+x}$ ($x \gtrless 0$) with y for the samples heated at low oxygen partial pressures. Heating temperature: 1200°C, Heating time: 50 h, □: $p_{O_2} = 10^{-15}$ atm, ○ and △: Different runs of $p_{O_2} \leq 10^{-19}$ atm.

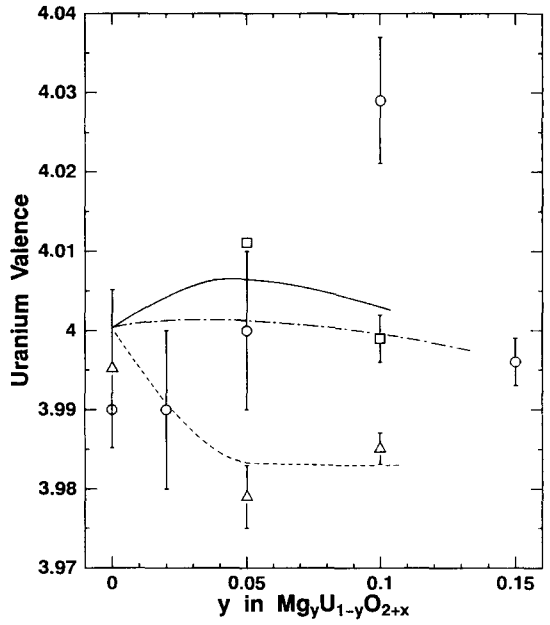

Fig. 2. Mean valence of uranium in $Mg_yU_{1-y}O_{2+x}$ plotted against y value. □: $p_{O_2} = 10^{-15}$ atm, ○ and △: Different runs of $p_{O_2} \leq 10^{-19}$ atm.

concentrations of foreign metal ions. It is also possible that magnesium is somewhat weak in letting the uranium ions take on higher oxidation states.

The above discussion was for the line connecting $x = 0$ at $y = 0$ and $x = -0.15$ at $y = 0.15$ in Fig. 1. The mean valence of uranium can be calculated for each set of (y, x) values by assigning $+2$ and -2 valences to magnesium and oxygen, respectively. Fig. 2 shows the mean valence as a function of y in $Mg_yU_{1-y}O_{2+x}$. The solid curve represents the change of the valence for $p_{O_2} = 10^{-15}$ atm, while the dash–dotted and dotted curves that for the different runs of $p_{O_2} \leq 10^{-19}$ atm. Due to large errors in

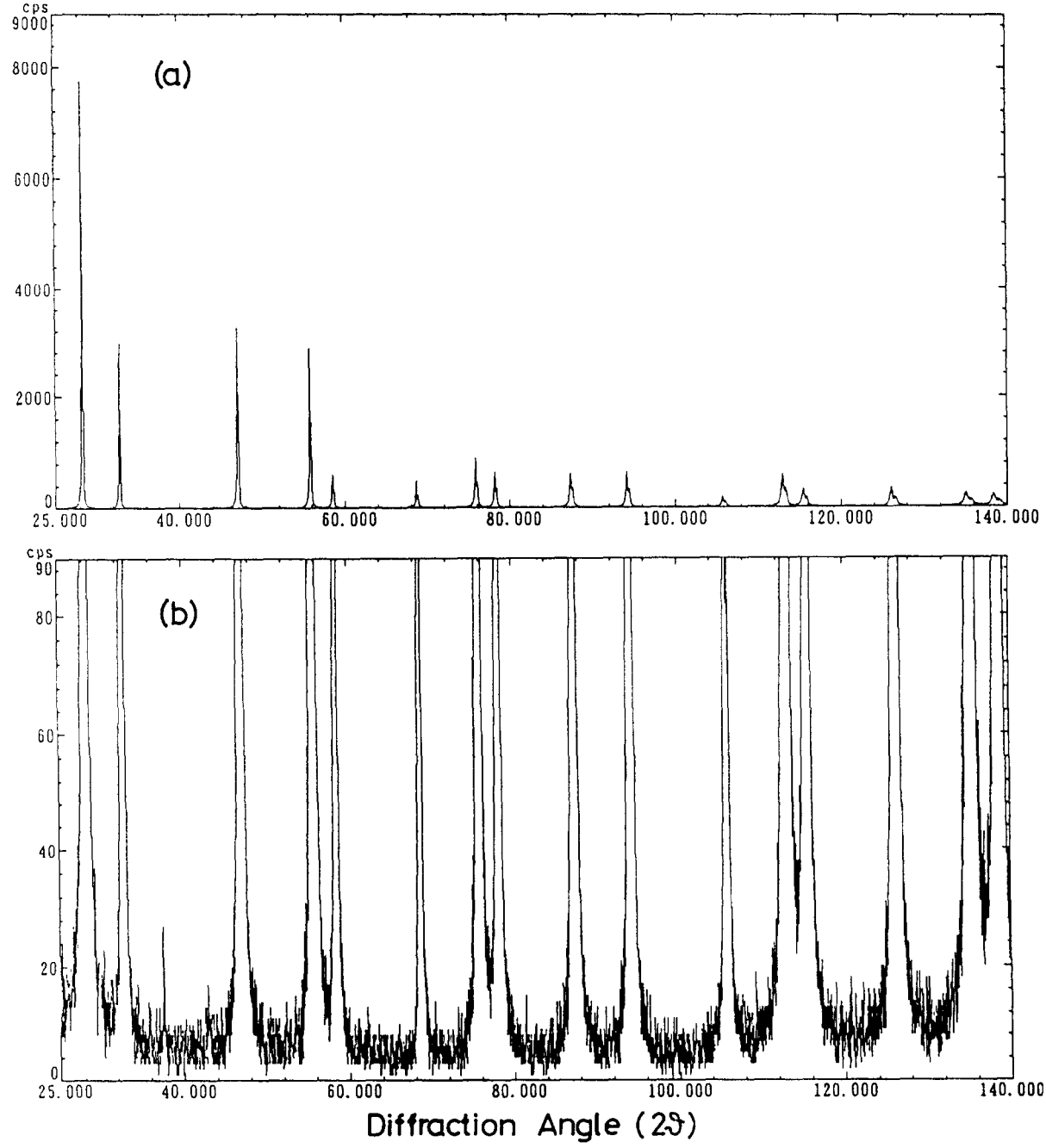

Fig. 3. X-ray diffraction pattern of the $y = 0.15$ sample heated at 1200°C under $p_{O_2} = 10^{-15}$ atm pressure giving only fcc lines. (a) Intensity range 9000 cps, (b) intensity range 90 cps. Scanning rate: 1°(2θ)/min.

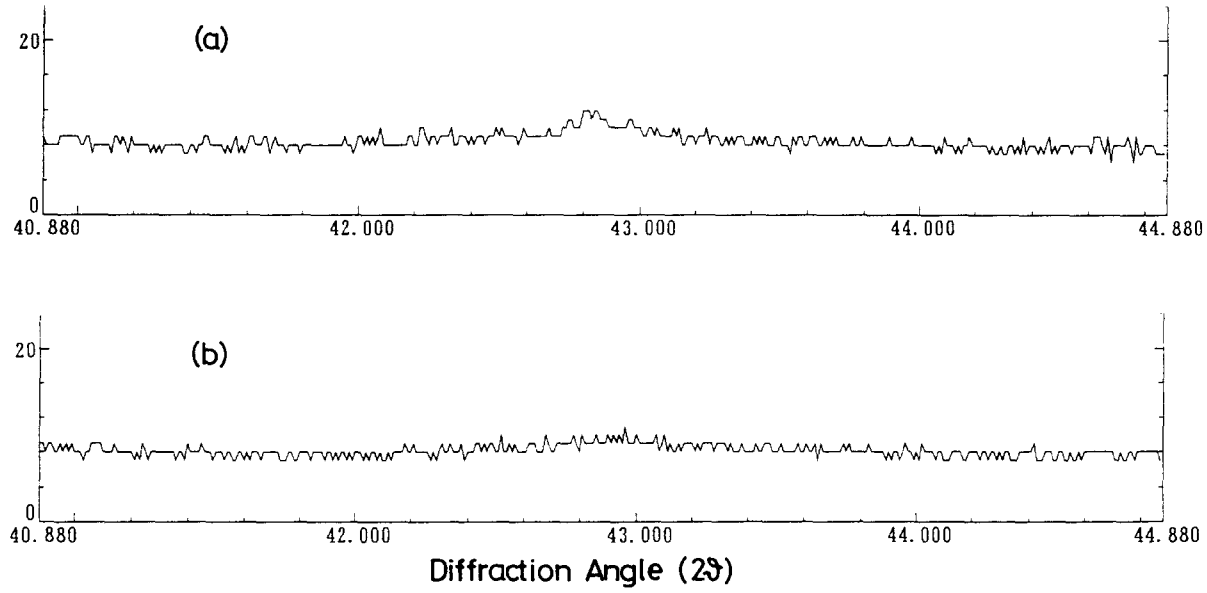

Fig. 4. Step scanned X-ray diffraction pattern with counting time 36 s and sampling width 0.01°. (a) $y = 0.15$, $p_{O_2} = 10^{-15}$ atm, (b) $y = 0.1$, $p_{O_2} = 10^{-15}$ atm.

the determination of uranium valence, the behaviour is obscure, but it is frequently the case that the mean valences are lower than +4 for the samples heated in the oxygen pressures $\leq 10^{-19}$ atm. The large separation of the circle and the triangle at $y = 0.1$ shows that the uranium valence is highly sensitive to the heating conditions.

The solubility of metal atom M in $M_yU_{1-y}O_{2+x}$ ($x \gtreqless 0$) is usually obtained from the break of a lattice parameter versus y plot. Actually for this solid solution, $Mg_yU_{1-y}O_{2+x}$, the solubility at higher oxygen pressures (e.g., 10^{-6} atm O_2) has been determined by this method [14]. However in the present case, the reproducibility of the lattice parameter was not so good that we obtained the magnesium solubility from the X-ray peaks of MgO phase which emerges from the fcc solid solution peaks above the solubility limit under the very low oxygen partial pressures [15–17]. Fig. 3(a) shows the X-ray diffraction pattern for $y = 0.15$ sample heated under $p_{O_2} = 10^{-15}$ atm. All the peaks are indexed to a fcc structure with lattice parameter, $a_0 = 5.4706$ Å. The same pattern for this sample is given in Fig. 3(b) with a magnified ordinate. The scanning rate was $1°(2\theta)$/min. If MgO is precipitated, the corresponding peaks should be observed. The ratio of signal to noise was, however, not high enough for that analysis. Then, the step scanning measurements were carried out counting 36 s for each 2θ angle with the sampling width of 0.01°. The X-ray diffraction pattern of the same sample is exhibited in Fig. 4(a) in the 2θ range from 40.88 to 44.88°. Although very weak, the strongest peak of MgO at 42.83° is distinctly seen in the pattern, i.e., the $y = 0.15$ sample is of a two-phase mixture. Fig. 4(b) is the step scanned pattern for $y = 0.1$ sample. In this case, no MgO peaks are observed. The same results were observed also for the samples heated at $p_{O_2} \leq 10^{-19}$ atm.

This X-ray peak analysis was carried out for other specimens heated under different oxygen partial pressures. The results are summarized in Fig. 5. It is seen from the figure that for the $y = 0.1$ sample the single-phase solid solution exists at two regions of oxygen partial pressures, namely above around $p_{O_2} = 10^{-6}$ atm and below 10^{-15} atm. Since the solid solution was also in the single phase at

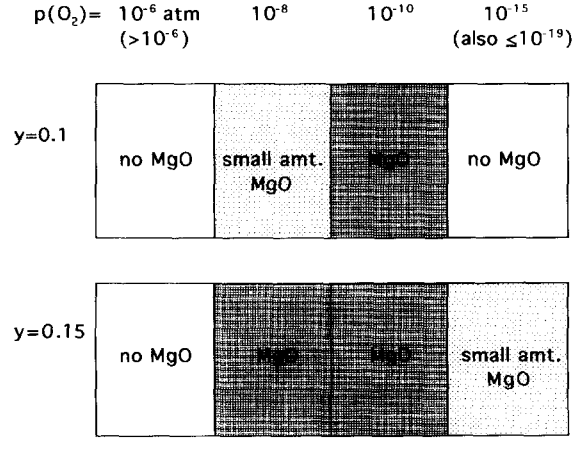

Fig. 5. Single-phase region of solid solution at 1200°C. Heating time: several times 50 h. Oxygen partial pressures of 10^{-6}, 10^{-8}, 10^{-10} and 10^{-15} atm were obtained by changing the CO_2/H_2 ratio, while that of $\leq 10^{-19}$ atm in H_2. White area: Single phase. Shaded area: Two phase mixture.

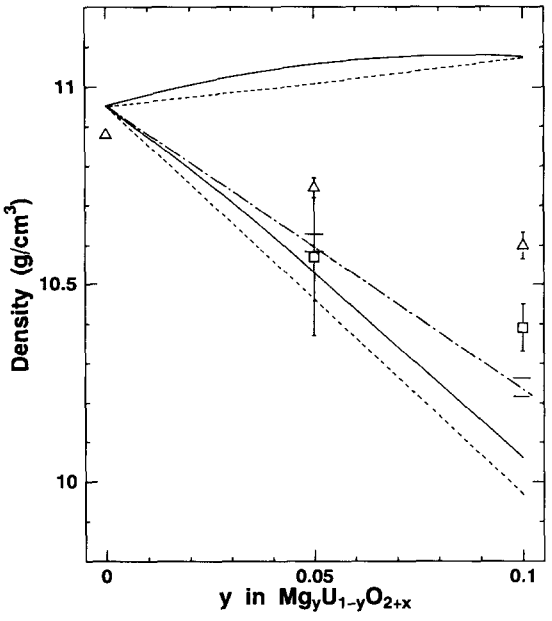

Fig. 6. Change of density with y in $Mg_yU_{1-y}O_{2+x}$. □: $p_{O_2} = 10^{-15}$ atm. △: $\leq 10^{-19}$ atm. ————: Theoretical lines for $p_{O_2} = 10^{-15}$ atm. ---: Theoretical lines for $p_{O_2} \leq 10^{-19}$ atm. For interstitial case, the density increases with increasing y, and for substitutional case it decreases with increasing y. – · – : Theoretical line for the mixture of MgO and UO_{2+x} ($x \gtrless 0$).

$p_{O_2} \leq 10^{-19}$ atm, it can be considered that the single phase region extends to a fairly wide range of low oxygen pressures below 10^{-15} atm. A two-phase region of the solid solution and MgO lies between the above two regions. For $y = 0.15$ sample, the single-phase solid solution exists at the region around $p_{O_2} = 10^{-6}$, but MgO precipitates in the solid solution phase though a small amount at $p_{O_2} = 10^{-15}$ and $\leq 10^{-19}$ atm. This result indicates that the solubility at 1200°C is between $y = 0.1$ and 0.15 for the lower region of oxygen partial pressure. The above experimental evidence that there are two single-phase solid solution regions for $y = 0.1$ and that the solubility is higher than $y = 0.1$ below the oxygen pressure of 10^{-15} atm is in good accordance with the transmission electromicroscopic observation, which is now in progress and the detailed description thereof will be made in a succeeding paper.

The separation of a single-phase solid solution into two regions of existence by a two-phase region between them does not seem to be usual. There is a possibility that the solid solutions in the two regions have the different type of solution structure. Here, we performed density measurements by the toluene displace method for four single-phase solid solutions of $y = 0.05$ and 0.1 heated under $p_{O_2} = 10^{-15}$ and $\leq 10^{-19}$ atm.

In Fig. 6, the measured density is plotted against y in $Mg_yU_{1-y}O_{2+x}$ ($x < 0$). The square and triangle marks express the data for $p_{O_2} = 10^{-15}$ and $\leq 10^{-19}$ atm, respectively. Each point is the average of three determinations. The solid and dotted lines show the theoretical change of the density with y for $p_{O_2} = 10^{-15}$ and $\leq 10^{-19}$ atm specimens, respectively. Since the measured lattice parameter is needed for calculating the theoretical density and it differs for the $p_{O_2} = 10^{-15}$ and $\leq 10^{-19}$ atm specimens, two lines (solid and dotted lines) appear for each of the substitutional and interstitial cases. The lines in Fig. 6 are those which were obtained by connecting smoothly the three theoretical densities for $y = 0$, 0.05 and 0.1. With increasing y, the theoretical density decreases for substitutional solid solution whilst it increases for interstitial solid solution.

The dash–dotted line in Fig. 6 shows the change of the theoretical density in the case where the product oxides were not the solid solution but the mixture of MgO and non-stoichiometric UO_{2+x} ($x \lessgtr 0$). The upper and lower horizontal bars of the two densities at $y = 0.05$ and 0.1 show the change of the density values with p_{O_2} for 10^{-15} and $\leq 10^{-19}$ atm samples, respectively. Except for the density of the $y = 0.05$ and $p_{O_2} = 10^{-15}$ atm sample, of which the error bar is much larger than those of the other three samples, the measured densities are significantly higher than the theoretical line for the mixture of MgO and non-stoichiometric UO_{2+x} ($x \lessgtr 0$). That is to say, the products are the solid solutions and not the mixture with MgO.

Another important point of the data is that the three observed densities are by far above the theoretical lines for substitutional solid solutions. The result can be explained if we consider that a part of the magnesium atoms enter into the interstitial sites as $(Mg_aU_{1-a})\{Mg_b\}O_{2+c}$, where the parentheses and the braces express the $4a$ metal atom sites and the $4b$ interstitial sites, respectively, in the unit cell of UO_2. In the above formula, the excess oxygen atoms would occupy the same interstitial sites if $c > 0$. This formula is related to the apparent formula of a substitutional type, $Mg_yU_{1-y}O_{2+x}$, by

$$(Mg_aU_{1-a})\{Mg_b\}O_{2+c} = (1+b)Mg_{(a+b)/(1+b)}U_{(1-a)/(1+b)}O_{(2+c)/(1+b)}. \quad (1)$$

That is to say

$$y = \frac{a+b}{1+b}, \quad (2)$$

and

$$x = \frac{2+c}{1+b} - 2. \quad (3)$$

The values of a, b and c were calculated by using the observed density and lattice parameter data. The density data were used for the calculation after correction for the closed pore. As is seen in Fig. 6, the observed density for

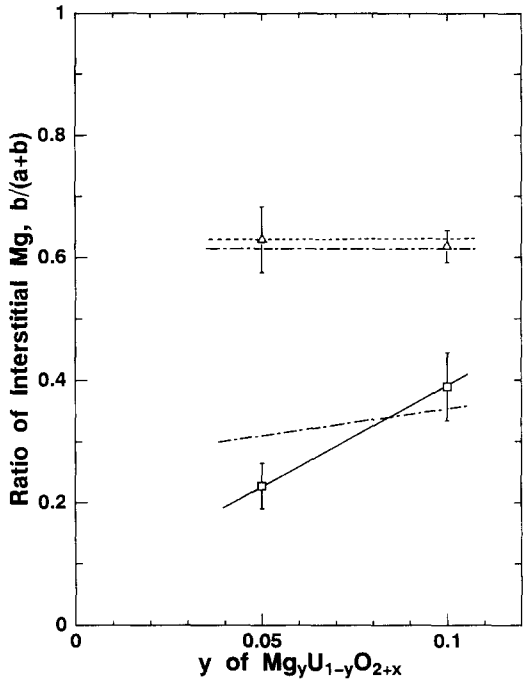

Fig. 7. Ratio of interstitial magnesium atoms to the total magnesium atoms against y of the apparent formula, $Mg_yU_{1-y}O_{2+x}$. □: $p_{O_2} = 10^{-15}$ atm, △: $\leq 10^{-19}$ atm. The dash–dotted lines are those from Eqs. (7) and (8).

$UO_{2.000}$ ($a_0 = 5.4710$ Å) was 10.879 g/cm^3 which is smaller than the theoretical density of the stoichiometric UO_2, 10.956 g/cm^3, by 0.077 g/cm^3. It is often mentioned that the observed densities are lower than the theoretical densities and the difference is generally ascribed to the closed pore [26] which cannot be displaced by toluene even by evacuation. Therefore, in this work the correction of the closed pore was carried out by adding 0.077 g/cm^3 to all the measured densities of solid solutions.

Fig. 7 shows the calculated ratio of interstitial magnesium to total magnesium ($R = b/(a+b)$) plotted against y of apparent formula $Mg_yU_{1-y}O_{2+x}$. The interstitial ratio increases with increasing y for $p_{O_2} = 10^{-15}$ atm, whereas it remains almost unchanged at higher ratios of ca. 0.6 for $p_{O_2} \leq 10^{-19}$ atm. It may be the case that the higher ratio cannot be realized in this solid solution.

The lattice parameter of solid solutions is mostly well represented by a linear equation of incorporated metal concentration and oxygen non-stoichiometry. For the magnesium solid solution prepared in higher oxygen partial pressures, the following relation has been obtained [14]:

$$a_0 = 5.4704 - 0.1170x - 0.5677y, \quad (4)$$

where the cubic lattice parameter, a_0, is given in Å. The modified equations connecting hyper- and hypo-stoichiometric regions were also presented [16]:

$$a_0 = 5.4704 - 0.0940x - 0.5577y + 0.055xy \quad (x \geq 0), \quad (5)$$

$$a_0 = 5.4704 - 0.7095x - 0.5577y \quad (x \leq 0). \quad (6)$$

The lattice parameter change with y of the apparent substitutional formula, $Mg_yU_{1-y}O_{2+x}$, is shown in Fig. 8. The data of each run form a line or a definite trend of change with y. The lattice parameters for $p_{O_2} = 10^{-15}$ atm (squares) are the lowest and those of two runs for $p_{O_2} \leq 10^{-19}$ (circles and triangles) never fall on the same line. It is difficult to express such a large difference by Eqs. (5) and (6). A natural deduction regarding this fact is that the interstitial magnesium atoms contribute to the lattice parameter change in a different manner from substitutional magnesium atoms. For $(Mg_aU_{1-a})\{Mg_b\}O_{2+c}$, the coefficients of a and c (≥ 0) were taken from Eq. (4) as -0.5677 and -0.1170, respectively. The coefficient of b was obtained by using the measured density data. The coefficient of c in the negative region was calculated with the above coefficients. The lattice parameter for $(Mg_aU_{1-a})\{Mg_b\}O_{2+c}$ is represented by

$$a_0 = 5.4704 - 0.5677a + 0.376b - 0.117c \quad (c \geq 0), \quad (7)$$

$$a_0 = 5.4704 - 0.5677a + 0.376b - 0.568c \quad (c \leq 0). \quad (8)$$

Eqs. (7) and (8) show that, in contrast to the substitutional magnesium, the interstitial magnesium atoms cause an

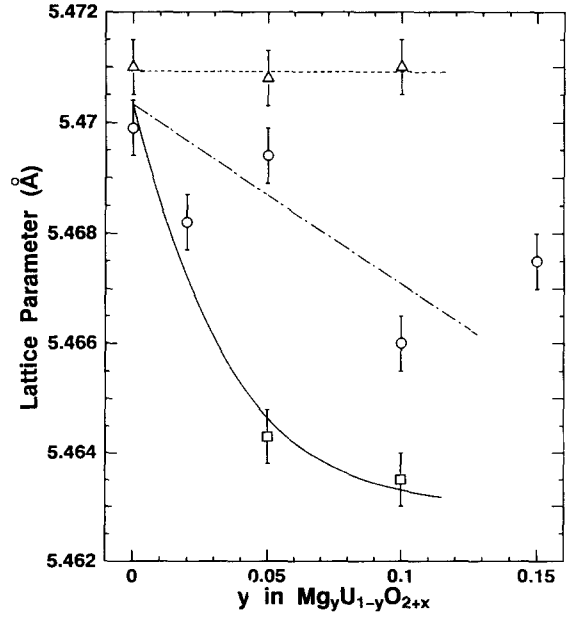

Fig. 8. Lattice parameters as a function of y of the apparent formula, $Mg_yU_{1-y}O_{2+x}$. □: $p_{O_2} = 10^{-15}$ atm. ○ and △: Different runs of $p_{O_2} \leq 10^{-19}$ atm.

Table 2
Values of a, b and c of $(Mg_aU_a)\{Mg_b\}O_{2+c}$ and the ratio of interstitial magnesium to total magnesium calculated with y, x and a_0

y	x	Lattice parameter, a_0 (Å)	a	b	c	Ratio of interstitial Mg, R	Remarks
0	-0.004 ± 0.01	5.4699	–	–	–	–	$\leq 10^{-19}$ atm O_2, ○
0.02	-0.026 ± 0.06	5.4682	–	–	–	–	$\leq 10^{-19}$ atm O_2, ○
0.05	-0.052 ± 0.007	5.4694	0.021	0.031	0.008	0.60	$\leq 10^{-19}$ atm O_2, ○
0.1	-0.087 ± 0.003	5.4660	0.043	0.064	0.035	0.60	$\leq 10^{-19}$ atm O_2, ○
0.15	-0.152 ± 0.001	5.4675	0.065	0.100	0.033	0.61	$\leq 10^{-19}$ atm O_2, ○ (MgO pptd.)
0	-0.002 ± 0.005	5.4710	–	–	–	–	$\leq 10^{-19}$ atm O_2, △
0.05	-0.060 ± 0.002	5.4708	0.020	0.032	0.002	0.61	$\leq 10^{-19}$ atm O_2, △
0.1	-0.107 ± 0.001	5.4710	0.039	0.067	0.021	0.63	$\leq 10^{-19}$ atm O_2, △
0.05	-0.045 ± 0.001	5.4643	0.035	0.016	−0.014	0.31	10^{-15} atm O_2, □
0.1	-0.100 ± 0.002	5.4635	0.068	0.036	−0.032	0.35	10^{-15} atm O_2, □

increase of the lattice parameter. The absolute value of the coefficient of c (≤ 0) in Eq. (8), 0.568, is seen to be fairly larger than those of the usual substitutional solid solutions, i.e., around 0.3 [27]. This may be because of the interstitial magnesium atoms present in this solid solution.

By the combination of Eq. (7) or Eq. (8) with Eqs. (2) and (3), the a, b and c values can be obtained from y, x and a_0. Calculation shows that there may be two solutions for the formula according to the input data. In Table 2, the acceptable set of the calculated values of a, b and c are listed together with the calculated ratio, R, of interstitial magnesium to the total magnesium in the solid solution. It may be noteworthy that not only negative c values but also positive ones are obtained for negative x values in Table 2 as a consequence of Eq. (3). The a, b and c values for the $y = 0.15$ sample can be used only for reference since this sample contains a small amount of MgO second phase. The errors in the lattice parameters are estimated to be within ± 0.0005 Å.

From Table 2 it is seen that the R values for $p_{O_2} \leq 10^{-19}$ atm are all 0.60–0.63 independent of the y value, which is in complete agreement with the R values obtained from density measurements. The R value for $p_{O_2} = 10^{-15}$ atm samples increases with a smaller slope from 0.31 for $y = 0.05$ to 0.35 for $y = 0.1$, but agreement is wholly good. The present calculation revealed that the c value makes a markedly sensitive response to the equilibrium with oxygen partial pressure causing the change of the lattice parameter to a significant order of magnitude. The scattering of the lattice parameter data is considered to be ascribable to the small change of the c value due to the incomplete attainment of equilibrium.

References

[1] J.C. Killeen, J. Nucl. Mater. 58 (1975) 39.
[2] K.C. Radford, J.M. Pope, J. Nucl. Mater. 116 (1983) 305.
[3] K.W. Song, S.H. Kim, S.H. Na, Y.W. Lee, M.S. Yang, J. Nucl. Mater. 209 (1994) 280.
[4] J.B. Ainscough, F. Rigby, S.C. Osborn, J. Nucl. Mater. 52 (1974) 191.
[5] J.C. Killeen, J. Nucl. Mater. 88 (1980) 177.
[6] P.T. Sawbridge, C. Baker, R.M. Cornell, K.W. Jones, D. Reed, J.B. Ainscough, J. Nucl. Mater. 95 (1980) 119.
[7] T. Matsui, K. Naito, J. Nucl. Mater. 136 (1985) 59.
[8] T. Tsuji, T. Matsui, M. Abe, K. Naito, J. Nucl. Mater. 168 (1989) 151.
[9] J. Tateno, T. Fujino, H. Tagawa, J. Solid State Chem. 30 (1979) 265.
[10] T. Fujino, N. Sato, J. Nucl. Mater. 189 (1992) 103.
[11] T. Fujino, N. Sato, K. Yamada, J. Nucl. Mater. 223 (1995) 6.
[12] H. Serizawa, T. Shiratori, K. Fukuda, T. Fujino, N. Sato, J. Alloys Compounds 218 (1995) 149.
[13] S. Kemmler-Sack, W. Rüdorff, Z. Anorg. Allg. Chem. 354 (1967) 255.
[14] T. Fujino, K. Naito, J. Inorg. Nucl. Chem. 32 (1970) 627.
[15] J.S. Anderson, K.D.B. Johnson, J. Chem. Soc. (1953) 1731.
[16] T. Fujino, J. Tateno, H. Tagawa, J. Solid State Chem. 24 (1978) 11.
[17] Hj. Matzke, private communication.
[18] H.R. Hoekstra, S. Siegel, E.X. Gallagher, J. Inorg. Nucl. Chem. 32 (1970) 3237.
[19] D. Jakes, I. Krivy, J. Inorg. Nucl. Chem. 36 (1974) 3885.
[20] K. Naito, T. Tsuji, S. Watanabe, H. Sakai, Solid State Ionics 3&4 (1981) 635.
[21] S.R. Dharwadkar, M.S. Chandrasekharaiah, Anal. Chim. Acta 45 (1969) 545.
[22] T. Fujino, T. Yamashita, Fresenius Z. Anal. Chem. 314 (1983) 156.
[23] D.E. Williams, Ames Lab. Rep. IS-1052, 1964.
[24] R. Braun, S. Kemmler-Sack, H. Roller, I. Seeman, I. Wall, Z. Anorg. Allg. Chem. 415 (1975) 133.
[25] S. Kemmler-Sack, I. Seeman, Z. Anorg. Allg. Chem. 409 (1974) 23.
[26] T. Fujino, J. Inorg. Nucl. Chem. 34 (1972) 1563.
[27] T. Fujino, C. Miyake, in: Handbook on Physics and Chemistry of the Actinides, Vol. 6, eds. A.J. Freeman and C. Keller (North-Holland, Amsterdam, 1990) p. 155.